Predicting the Composition of Qurna Crude Oil Fraction by Ternary Composition Diagram

Harith H. Al-Moameri*†, Ghanim Hassan‡, Mohammed Ali Abdulrehman†

†Materials Engineering Department, University of Mustansiriyah, Baghdad, Iraq; *e-mail: almoamerih@uomustansiriyah.edu.iq
‡Middle Technical University, Baghdad, Iraq.

Recieved: July 09, 2019; Accepted: April 11, 2020
DOI: 10.17721/moca.2020.33-39

With a goal to identify, and ultimately removing from the oil fraction, the carcinogenic components, an oil fraction oil has been analyzed into a main three hydrocarbon groups, paraffins, aromatics, and polycyclic saturates. A multi-stage adsorption apparatus has been used. Four units of 300 g alumina each seems to be sufficient for removing the polynuclear aromatics from 75 g of an oil fraction boiling between 365-375 °C from Qurna crude oil. The usefulness of the ternary diagram for analyzing the oil fraction to the three hydrocarbons groups has been studied and verified. An experimentally based linear relationship of density and refractive index was established to enable of identifying the composition of an oil fraction using the values on refractive index alone. Separation of uncontaminated paraffins requires higher adsorbent/oil ratio and/or more significant number of adsorption units. Ensuring no overloading of the adsorbent was essential for the separation.

Keywords: adsorption, chemical analysis, prediction, separation, model

Adsorption has been widely employed commercially for separation and purification of a wide range of gases and liquids. In crude oils and oil fractions, different hydrocarbon groups have different absorbability on the adsorbent surface [1-2]. Activated alumina, activated carbon, and silica-gel are widely used as adsorbents for the separation in petrochemical and general chemical industries. Commercial application of adsorption includes air drying, recovery of solvents, de-colorization of aqueous sugar solutions, and fractionation of hydrocarbons from crude oil [3-5].

The first appearance of adsorption dates back to a mid-eighteens century when F. F. Runge separated certain colored materials into zones on filter paper. Later, D. T. Day separated crude oils into various fractions by passing through pulverized fuller earth [6-7]. Later, many researchers focus on the investigating methods for experimentally analyzing crude oil and oil fractions [8-9].

Polynuclear aromatics was found to be mainly associated with the biological activity of the mineral oils. For years, researchers were working on isolating and identifying carcinogenic compounds directly from crude mineral oils, although, no pure carcinogen component was isolated [10-11].

Dynamic simulation was developed by Ren for characterization molecular size of heavy crude oil fractions and identifying polycyclic aromatic content [12]. Liquid-Solid Adsorption Chromatography was used to fractionation of two kinds of crude oil into eight fractions each. Brown-Ladner method obtained from H-NMR data and molecular weight to predict the molecular structures and the content of polycyclic aromatic. The results from this research show that the content of polycyclic aromatic increases with increasing the molecular weight of the oil fraction.

An analytical chemistry method for identifying carcinogenic hazard of aromatic hydrocarbons was developed by a relationship between carcinogenicity and mutagenicity index (MI), polycyclic aromatic content (PAC) ring content, and gas-chromatographic distillation curves of the oil fractions. A linear relationship between MI and PAC ring content were obtained [13].

Jia et al studied the pyrolysis of oil shale in a laboratory two-stage fluidized bed to identify oil composition and quality. A 50 % heavy fraction boiling above 350 °C was obtained and was disappeared at temperatures above 550 °C after adding fluidized bed as secondary cracking resulting increasing of paraffins and other light fractions [14].

Costa et al. [15] synthesized a new mesoporous adsorbent to remove polycyclic aromatic hydrocarbons. The adsorbent was characterized by FTIR, XRD, N_2 adsorption/desorption, SEM, TGA, and EDX analyses and the material shows the high surface area, uniform mesopore size distribution, and thermal stability when removing two polycyclic aromatic hydrocarbons (PAH) components that were employed for testing the efficiency of absorption.

Ugochukwu et al. [16] studied the removing of PAH from crude oil through adsorption and biodegradation by performing experiments in aqueous clay/oil systems. The results show that the clay/oil system with high cation exchange capacity was not stimulatory to biodegradation of crude oil PAH compounds. Further research by Ugochukwu [17] was focusing on the effect of acid-activated clay minerals where the results show that the acid-activated clays did not improve the biodegradation of the PAH.

A particle size distribution and chemical composition of the petrochemical wastewater discharges of China National Offshore Oil Corporation was made to build the chemical oxygen demand and biochemical oxygen demand fingerprints with a goal for removing toxic substances [18]. The step by step filtration method and molecular weight classification method techniques were adopted. It was found that the primary pollutants were settleable particles in petrochemical wastewater.

With a goal to identify the carcinogenic components in heavy crude oil fractions, Qurna crude oil was distilled under reduced pressure to ensure no permanent changes of the oil composition or properties. Oil fractions were collected and the oil fraction boiling between 365-375 °C (hereafter referred to as $F_{365\text{-}375}$) was found the most active biologically and polycyclic aromatics hydrocarbons were mainly responsible for the carcinogenic behavior. The usefulness of a multi-stage adsorption apparatus for the separation of mineral oil into paraffin, aromatics, and polynuclear saturates groups was presented and asserted its potential to the industrial application for the continuous production of safe oils [19]. The method was aimed to obtain maximum information of the oil fraction considering aromatics, paraffinic, and polycyclic saturates are the only constituents.

The method of analysis uses repeated chromatographic separation to isolate and identify theses key components in $F_{365\text{-}375}$ oil fraction using the limiting values of density and refractive index. A ternary diagram was constructed on the basis of density and refractivity intercept and the constituent of aromatics, paraffinic, and polycyclic saturates were calculated from the base, left, and right axis respectively. The ternary diagram of this research was adopted in many literatures before [20-22].

Experimental part

The oil fraction separated in this research has a boiling point ranged from 365 to 375 °C ($F_{365\text{-}375}$) obtained by the distillation of Qurna crude oil. A semi-automatic crude oil distillation apparatus from BR Instruments Inc. was used.

Iso-octane was used as a solvent and methanol was used to wash off the alumina from compounds not absorbable by iso-octane. Iso-octane was found to be the more suitable solvent for the separation of mineral oils. The physical properties of this oil fraction and the solvents were measured and tabulated in Table 1.

Table 1. Properties of $F_{365\text{-}375}$ and solvents.

Properties at 25 °C	Value	Iso-octane	Methanol
Density, g/mL	0.9731	0.6197	0.794
Refractive index	1.5488	1.388	1.3269
Viscosity, cp	40.1	-	-
Boiling point, °C	-	99.48	64.6

The results of $F_{365\text{-}375}$ characterization on the ternary composition result 55 % aromatics, 45 % polycyclic aromatics, and 0 % paraffin.

Alumina, manufactured by Delta Enterprises Inc., was used as an adsorbent. The analysis shows that the mesh number is 100-200, pour volume 0.261 mL/g, pore diameter 70 Å, surface area 145 m^2/g, and bulk density of 1.041 g/mL.

The solvent was removed from the samples by using rotary film evaporator, supplied from Shiva Scientific Glass Pvt. Ltd., associated with a water bath (60-70 °C) and connected to a vacuum system (vacuum pump from Gardner Denver, Inc.). The solvent was condensed and collected in a flask. Abbe-60 ED refractometer, form Keison Products, with a prism temperature within 0.1 °C was used to measure the refractive index of the oil samples.

A semi-continuous multistage separation apparatus was found by previous studies to be a more practical alternative to column or batch separation for mineral oils [23-24].

The Multi-stage apparatus (Plates#1 and #2) consists of five glass units (stages) 6” high and 4” diameter each. The lower section leads to a two-way glass tap (plate#3). A stirrer was fitted to the endplate of each unit and a speed of 250 rpm was found satisfactory.

The solvent feed system is shown in **Figure 1**. It consists of a spherical solvent reservoir and two cylindrical solvent feed tanks. Nitrogen was supplied to the apparatus from a cylinder fitted with a needle valve.

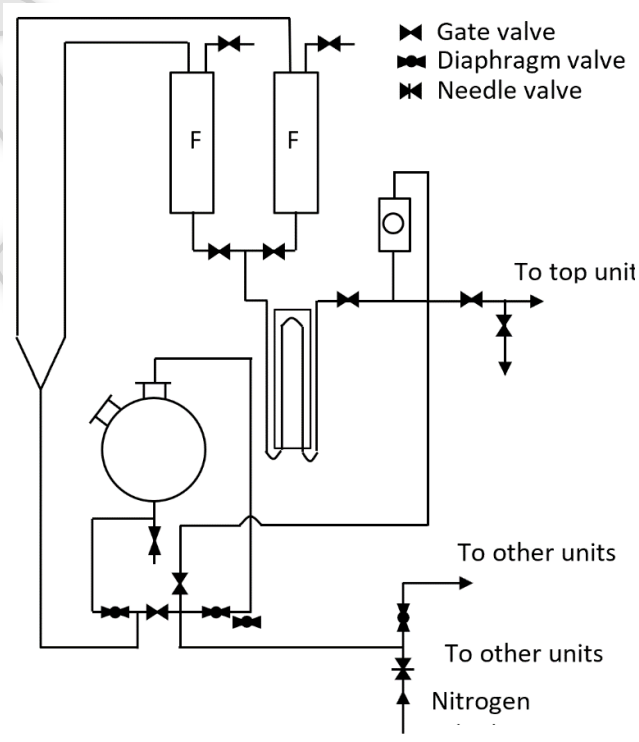

Fig. 1. Process flow diagram of feed system of the multi-stage apparatus.

The $F_{365-375}$ oil sample was added to the top unit which was stirred for 160 minutes (the equilibrium time), and the solution was allowed to overflow to the rest of the units. The solvent was continuously fed to the top unit in a steady flow rate for each experimental run. The samples were collected from the bottom unit and stripped from the solvent, weighted, and analyzed for density and refractive index.

Results and Discussion

Series of runs of the multi-stage apparatus (Run#1 to Run#4) was performed using the same amount of oil in the top unit and approximately the same flow rate. An additional run (Run#5) was performed to exclude any overloading of the adsorbent in the top unit. Table 2 shows the experimental conditions of each run.

Figure 2 shows the experimental results of the weight fraction of the oil recovered from the five runs versus the cumulative effluent volume and Table 3 show percent recoveries of these runs. The higher recoveries from Run#3 and Run#4 may be attributed to the "mechanical" displacement of the polynuclear aromatics with the oil solution rather than being retained on the gel. This displacement is caused by the increasing overloading of the adsorbent (alumina) to oil ratio is decreased.

Run#5 is generally shown different results compared to other runs as it was designed to avoid any overloading of the adsorbent. The large adsorbent/oil ratio (60:1) of this run allows better separation where all the polynuclear aromatics are retained by the gel resulting in lower iso-octane and methanol recoveries. The availability of the adsorbent enhances the retention of mono- and di-nuclear aromatics and some of the polycyclic saturates that are not held by the adsorbent in more competitive conditions of lower adsorbent/oil ratios. The high oil recovery of Run#5 (99.2 %) is attributed to the easier washing by methanol in view of the low amount of oil on the gel.

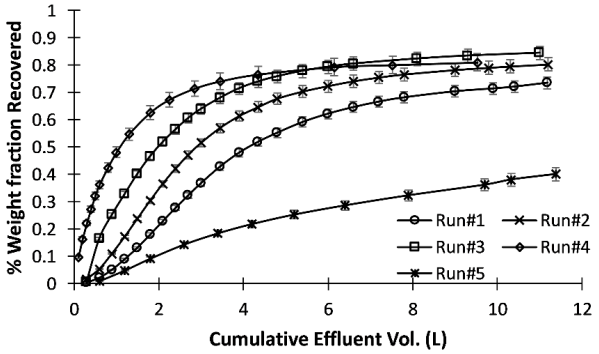

Fig. 2. The weight fraction of recovered oil vs cumulative effluent volume. Circle, cross, square, diamond, and star symbols refer to Runs#1 to #5 respectively.

Table 2. Experimental conditions of each run.

Conditions		Run#1	Run#2	Run#3	Run#4	Run#5
Weight of oil in top unit (g)		75	75	75	75	15
Flow rate (mL/min.)		2.65	2.38	2.35	2.34	2.51
Unit#1	alumina (g)	300	300	300	300	300
	solution (g)	500	900	900	900	800
Unit#2	alumina (g)	300	300	300	-	300
	solution (g)	650	500	900	-	1100
Unit#3	alumina (g)	300	300	-	-	300
	solution (g)	430	900	-	-	600
Unit#4	alumina (g)	300	-	-	-	-
	solution (g)	700	-	-	-	-
Unit#5	alumina (g)	-	-	-	-	-
	solution (g)	-	-	-	-	-

Table 3. % Recovery of the oil fraction.

Runs	No. of Units	Iso-octane recovery	Methanol recovery	Total recovery	Adsorbent/oil Ratio
Run#1	4	71.3	21.3	92.6	16:1
Run#2	3	75.5	10.3	85.8	12:1
Run#3	2	81.1	10.5	91.6	8:1
Run#4	1	76.9	6.6	83.5	4:1
Run#5	3	38.2	61	99.2	60:1

The progress of the separation of the oil fraction in the five runs is followed by plotting the refractive index versus percentage oil recovered of the oil (weight fraction of the oil recovered) as shown in **Figure 3**. The removal of the last one, two, three, and four units from 5-cascade results in a progressive deterioration of the separation. The paraffinic content of the early samples was correspondingly reduced on the removal of further units, as shown in Table 4 in which the lowest and highest refractive indices of each run are given.

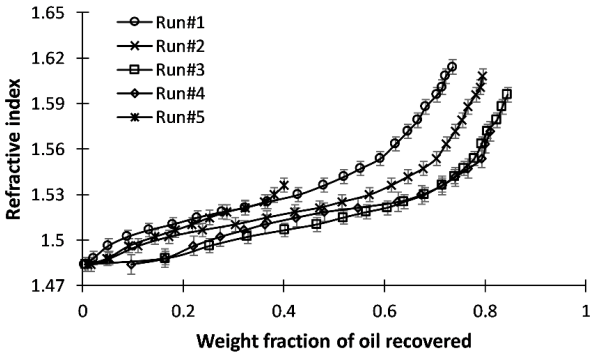

Fig. 3. Refractive index versus the weight fraction of the oil recovered. Circle, cross, square, diamond, and star symbols refer to Runs#1 to #5 respectively.

Table 4. Lower and higher values of the refractive index of the oil samples.

Runs	No. of Units	Lowest nD25	Highest nD25
Run#1	4	1.469 (45.0 % Par.)	1.6241
Run#2	3	1.4221 (41.5 % Par.)	1.6257
Run#3	2	1.5270 (18.5 % Par.)	1.6288
Run#4	1	1.5295 (3.0 % Par.)	1.615
Run#5	3	1.4608 (88.0 % Par.)	1.601

The refractive index of oil samples obtained from the five runs was plotted against its density as shown in **Figure 4**. This plot depicts the experimentally found correlation between the refractive index and the density of the $F_{365\text{-}375}$ oil fraction (Equation 1).

$$D_{en.} = 1.3776 * N - 1.2064 \qquad \text{Equation 1}$$

The importance of this equation lies in its simplification of the use of ternary composition diagram where density is no longer needed, and the composition is defined by refractive index alone. The validity of this relationship comes from the narrow boiling range of the oil fraction (365-375 °C) and the relatively low complexity in a chemical structure which allows averaging of the physical properties. The separation of the oil fraction ($F_{365\text{-}375}$) was followed on the hydrocarbon-type ternary composition diagram (Aromatics, paraffinic, and polycyclic saturates) as shown in **Figure 5**. The separation proceeds along curves extending from 10 % paraffin point on the Aromatic-Paraffinic side to the 50 % Aromatic point on the Aromatic-Polycyclic saturates side and then along the Aromatic-Polycyclic saturates side toward the 100 % Aromatic point. The larger the number of separation stages employed, the better the separation becomes and the more paraffinic the first oil samples obtained in the run are. Run#5 shows more efficient separation in terms of achieving the most paraffinic oils. The ternary diagram shows that the first samples of an efficient separation to be free of polycyclic saturates (see the aromatic-paraffin line).

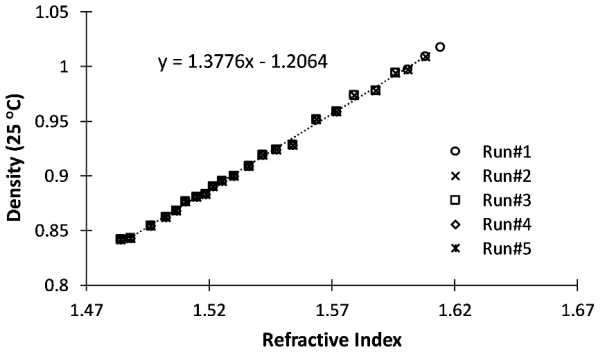

Fig. 4. Refractive index versus density of oil samples. Circle, cross, square, diamond, and star symbols refer to Runs#1 to #5 respectively.

Fractions of aromatics, paraffinic, and polycyclic saturate were also plotted against the percent oil recovered for the five runs as shown in **Figure 6**. The area under each curve of these plots represent the number of aromatics, paraffinic, and polycyclic saturates recovered from the oil samples. The plots show the order of efficiency of separation where Run#5 > Run#1 > Run#2 > Run#3 > Run#4. It was also shown that for most of the intermediate-range of separation (15-50 % recovery range), the oil samples collected contained 47-50 % polycyclic saturates while percentages of paraffinic and aromatics continued to fall and rise respectively.

The oil samples recovered by the use of methanol were generally found to consists of 100 % aromatics. Assuming the oil not recoverable by iso-octane or methanol to be 100 % aromatics, the resulting mass balance over individual compound groups are shown in **Table 5**.

The results of this mass balance show underestimation of paraffin and overestimation of polycyclic saturates as the adsorbent/oil ratio decreased in the first four runs. This is attributed to the fact that low adsorbent/oil ratios result in poor separation whereby the paraffin and polycyclic aromatics compounds rather than being separated from the aromatics group are distributed into a much larger number of predominantly aromatic samples which led to too low concentration. The ternary diagram of **Figure 5**; however, gives more accurate estimations of aromatic content vis an average of 64.35 % excluding Run#5.

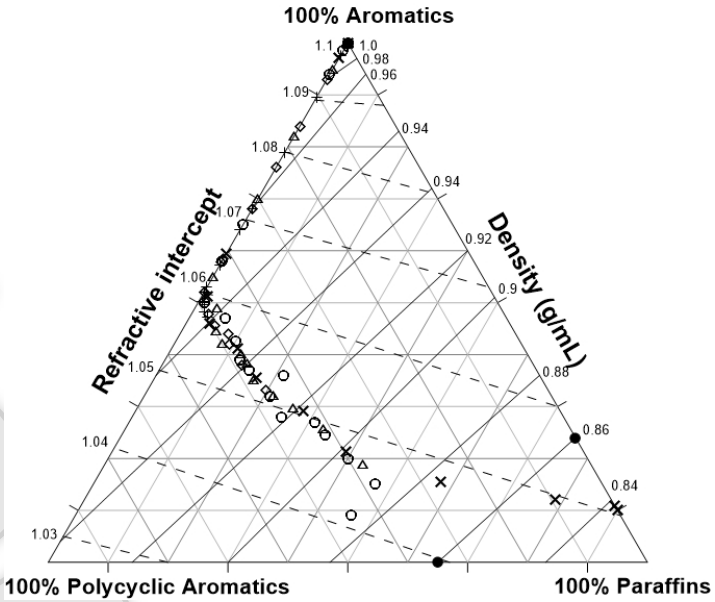

Fig. 5. Tertiary composition diagram for hydrocarbon analysis. Straight and dash lines refer to density and refractive intercept respectively. Circle, cross, square, diamond, and star symbols refer to Runs#1 to #5 respectively.

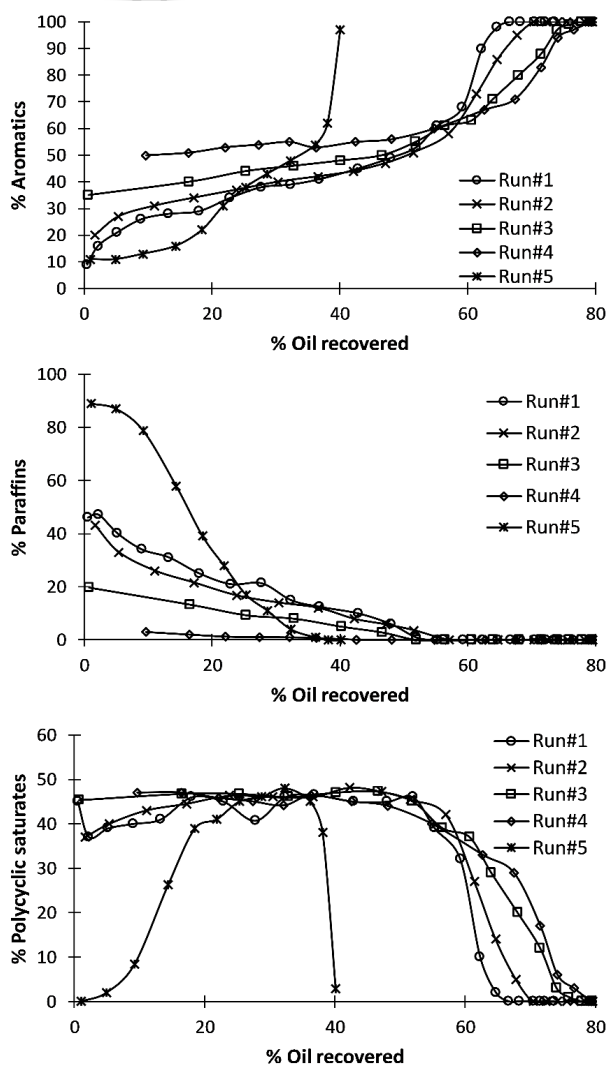

Fig. 6. Hydrocarbon analysis of the oil fraction. Circle, cross, square, diamond, and star symbols refer to Runs#1 to #5 respectively.

Table 5. Mass Balance of oil fraction.

Runs	Amount (g)			The composition of the oil sample, %		
	Oil	Paraffins	Polycyclic Aromatics	Paraffins	Aromatics	Polycyclic Aromatics
Run#1	75	7	20	9.33	64.00	26.67
Run#2	75	5.5	22	7.33	63.33	29.33
Run#3	75	3.1	24	4.13	63.87	32.00
Run#4	75	0.35	25	0.47	66.20	33.33
Run#5	15	2.05	3	13.67	66.33	20.00
Average (Run#1 to Run#4)	-	-	-	5.32	64.35	30.33

The high Sulphur content in the oil fraction may results overestimation of the aromatic groups in the oil samples. However, this is recommended to further research.

The main purpose of this research was to separate the polynuclear aromatic compounds which contain the carcinogenic agents. Based on the results, this can be achieved using alumina with less stringent conditions of separation process without using high adsorbent/oil ratios and using a large number of separate units for isolating paraffinic compounds. From the results above, using four separation units each having 300 g alumina is sufficient to separate the polynuclear aromatics from a 75 g oil sample.

Ultraviolet spectroscopy (UV) was used to validate the analysis of hydrocarbon type followed in this research (**Figure 7**). Saturates compound do not absorb in the UV, and the shape of the UV curves represent mainly the constitution of the aromatic compounds while the position of the spectra on the ordinate represents the proportion of these compounds.

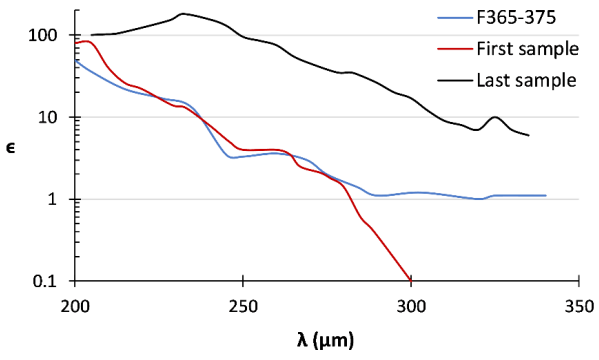

Fig. 7. UV Spectra for $F_{365\text{-}375}$ and first and last samples of Run#1.

The complexity of the high-boiling oil fraction used permits only for the qualitative indication for the board types of aromatic compounds.

The UV spectra were obtained for the oil fraction ($F_{365\text{-}375}$) and the first and last samples obtained from the first run. The first sample shows low aromatic content while the last sample shows higher aromatic content than the oil fraction, thus, generally corroborating the results obtained using the ternary composition diagram for analyzing those oil as shown in Table 6. The broadband at 270 mμ of the last sample indicates the presence of single ring aromatics. This peak is generally absent from other curves indicating that the aromatic compounds are generally polycyclic.

Table 6. The composition of oil fraction and first and last samples of Run#1 using UV.

Sample	% Paraffins	% Aromatics	% Polycyclic aromatics
$F_{365\text{-}375}$	0	59	41
First	44	10	46
Last	0	100	0

Conclusions

The composition of $F_{365\text{-}375}$ oil fraction to aromatics, paraffinic, and polycyclic saturates followed to identify and ultimately removing, the carcinogenic components.

A multi-stage apparatus was used in the separation process. Four units of 300 g alumina each were found sufficient for the separation of polycyclic aromatics for 75 g of $F_{365\text{-}375}$. These results are significant for removing of carcinogenic components form mineral oil.

A linear relationship was found to exists between the densities and refractive indices of the samples obtained from the multi-stage adsorption process. This relationship simplifies the use of the ternary composition diagram since only the measurement of the refractive index is needed for obtaining the hydrocarbon composition.

The current research will be the base for a simulation project of the adsorption process aiming to predict the constituents of the oil fraction.

Conflicts of interest

There are no conflicts to declare.

Acknowledgements

The authors would like to thank Mustansiriyah University (www.uomustansiriyah.edu.iq) Baghdad-Iraq for its support in the present work.

References

1. Basmadjian, D., *Mass Transfer and Separation Processes: Principles and Applications*. 2 ed. 2007, Boca Raton CRC Press.
2. Seader, J.D., E.J. Henley, and D.K. Roper, *Separation Process Principles: Chemical and Biochemical Operations*. 3 ed. 2011, Hoboken, NJ: John Wiley & Sons.
3. Seader, J.D. and E.J. Henley, *Separation Process Principles, 2nd Edition, Scader & Henley, 2006: Separation Process Principles*. 2 ed. 2006: John Wiley & Sons, Inc.
4. Ramaswamy, S., H. Huang, and B. Ramarao, *Separation and Purification Technologies in Biorefineries*. 2013, NY, USA: John Wiley & Sons, Ltd.
5. Kirk, R.E., D.F. Othmer, and R. Agrawal, *Kirk-Othmer Separation Technology*. 2 ed. 2008, NY, USA: Wiley-Interscience.
6. Varjani, S.J., E. Gnansounou, and A. Pandey, Comprehensive review on toxicity of persistent organic pollutants from petroleum refinery waste and their degradation by microorganisms. *Chemosphere*, 2017. **188**, 280-291.
7. Kolomnikov, I.G., et al., Early stages in the history of gas chromatography. *J Chromatogr A*, 2018. **1537**, 109-117.
8. LÜ, G., et al., The Adsorption of Phenol by Lignite Activated Carbon. *Chinese Journal of Chemical Engineering*, 2011. **19**(3), 380-385.
9. Jin, H., et al., Gas–Liquid Mass Transfer Characteristics in a Gas–Liquid–Solid Bubble Column under Elevated Pressure and Temperature. *Chinese Journal of Chemical Engineering*, 2014. **22**(9), 955-961.
10. Teutenberg, T., Potential of high temperature liquid chromatography for the improvement of separation efficiency—A review. *Analytica Chimica Acta*, 2009. **643**(1), 1-12.
11. Bai, S., et al., Protein adsorption onto diethylaminoethyl dextran modified anion exchanger: Effect of ionic strength and column behavior. *Chinese Journal of Chemical Engineering*, 2018. **26**(2), 259-267.
12. Ren, W., et al., Molecular size characterization of heavy oil fractions in vacuum and solution by molecular dynamic simulation. *Frontiers of Chemical Engineering in China*, 2010. **4**(3), 250-256.
13. Goyak, K.O., et al., Development of a screening tool to prioritize testing for the carcinogenic hazard of residual aromatic extracts and related petroleum streams. *Toxicol Lett*, 2016. **264**, 99-105.
14. Tian, Y., et al., Characteristics of oil shale pyrolysis in a two-stage fluidized bed. *Chinese Journal of Chemical Engineering*, 2018. **26**(2), 407-414.
15. Costa, J.A.S., et al., Efficient adsorption of a mixture of polycyclic aromatic hydrocarbons (PAHs) by Si–MCM–41 mesoporous molecular sieve. *Powder Technology*, 2017. **308**, 434-441.
16. Ugochukwu, U.C. and C.I. Fialips, Crude oil polycyclic aromatic hydrocarbons removal via clay-microbe-oil interactions: Effect of acid activated clay minerals. *Chemosphere*, 2017. **178**, 65-72.
17. Ugochukwu, U.C. and C.I. Fialips, Removal of crude oil polycyclic aromatic hydrocarbons via organoclay-microbe-oil interactions. *Chemosphere*, 2017. **174**, 28-38.
18. Jia, X., et al., Characterization and analysis of petrochemical wastewater through particle size distribution, biodegradability, and chemical composition. *Chinese Journal of Chemical Engineering*, 2019. **27**(2), 444-451.
19. Fornstedt, T., Characterization of adsorption processes in analytical liquid–solid chromatography. *Journal of Chromatography A*, 2010. **1217**(6), 792-812.
20. Gooding, R.M., N.G. Adams, and H.T. Rall, Determination of Aromatics, Naphthenes, and Paraffins By Refractometric Methods. *Industrial & Engineering Chemistry Analytical Edition*, 1946. **18**(1), 2-13.
21. Riazi, M.R. and T.E. Daubert, Prediction of the Composition of Petroleum Fractions. *Industrial & Engineering Chemistry Process Design and Development*, 1980. **19**(2), 289-294.
22. Pande, S.G. and D.R. Hardy, Evaluation of refractivity intercept as a method for determining fuel composition according to hydrocarbon type. *Fuel*, 1992. **71**(2), 231-235.
23. Miller, J.M., *Chromatography: Concepts and Contrasts*. 2009, Hoboken, NJ: John Wiley & Sons, Inc.
24. Speybrouck, D. and E. Lipka, Preparative supercritical fluid chromatography: A powerful tool for chiral separations. *Journal of Chromatography A*, 2016. **1467**, 33-55.